

Cosmological Implications of the GWTC-3 Modified-Propagation Anomaly: Inference Bias in the Hubble Tension

Aiden B. Smith
Independent Researcher
(Dated: February 10, 2026)

We investigate cosmological implications of the GWTC-3 O3 modified-propagation anomaly with an updated Planck-facing calibration chain. A 60-restart Planck+MG refit defines a revised sound-horizon anchor with posterior medians $H_0^{\text{Planck, MG}} \approx 68.01$, $\Omega_m^{\text{Planck, MG}} \approx 0.3064$, and $A_{\text{lens}} \approx 1.043$.

The leading result is inference bias: if modified-gravity truth is analyzed with GR standard-ruler compression, recovered H_0 shifts by mean $\Delta H_0 = +1.88 \text{ km s}^{-1} \text{ Mpc}^{-1}$ (fixed Ω_m) or $+4.55 \text{ km s}^{-1} \text{ Mpc}^{-1}$ (lensing-proxy Ω_m), i.e. order +2 to +5 $\text{km s}^{-1} \text{ Mpc}^{-1}$ relative to draw-level truth.

Direct late-time friction closure is weaker. After rebasing constrained transfer sweeps, the anchor-relief posterior is $\mathcal{R}_{\text{anchor}}^{\text{GR}} = 0.155$ (mean; $p16/p50/p84 = 0.108/0.147/0.189$), about 15% of the local-versus-Planck baseline gap.

For CMB lensing, baseline CAMB propagation predicts suppressed power at $L \sim 100$ and $L \sim 300$ (-15.3% and -9.5% medians). An MG-aware response refit restores near-reference quality (median $\chi^2 = 8.06$ versus 9.04 for the Planck reference).

A forward amplitude dial, $R_\alpha(z) = 1 + \alpha [R(z) - 1]$, gives a compact sensitivity map: core cross-channel support appears at $\alpha \approx 0.6$, while a material-relief threshold of 0.30 is reached near $\alpha \approx 1.94$ under linear relief coupling. A quick nonlinear bridge scan finds viable late-transition families, e.g. $(\alpha_{\text{high}}, \alpha_{\text{low}}, z_t, w) \approx (0.60, 1.95, 0.26, 0.03)$, that satisfy both core gates and material-relief targets.

Ancillary predictive checks are directionally consistent but mixed: Pantheon SN-only transfer gives a weak positive Bayes factor ($\log \text{BF} \approx +0.24$), while the all-transfer variant is mildly negative ($\log \text{BF} \approx -0.48$). Hero-event leave-one-out for the O3 injection-logit run gives $\Delta \text{LPD} = 3.67 \rightarrow 2.19$ after removing GW200308_173609, indicating concentration without single-event collapse. These results motivate full re-inference with larger siren samples.

I. SCOPE AND FRAMING

This work treats the O3 modified-propagation signal phenomenologically: given the inferred posterior, what cosmological consequences follow? The O3 anomaly analysis and data products are archived on Zenodo [1]. We do not re-argue detection significance in this manuscript.

Modified GW propagation has been explored in theory-forward frameworks [15, 16]. In this follow-up, we assume the running effective Planck mass $M_*(z)$ associated with GW friction is a universal MG sector ingredient, so the same $M_*(z)$ trajectory also modifies the background/scalar channels probed by CMB compression and lensing [17, 18]. Here, we use a data-driven posterior and update the pipeline to answer three questions in one chain:

1. How much late-time Hubble tension relief remains after recalibrating the sound-horizon calibration anchor?
2. Does Planck 2018 lensing necessarily reject this posterior, or can an MG-aware refit absorb the suppression?
3. How much can GR-based standard-ruler inversion bias inferred H_0 if MG truth is assumed?

II. PIPELINE SUMMARY

Posterior draws are taken from `outputs/finalization/highpower_multistart_v2/M0_start101` and propagated through four linked stages:

1. **Global Planck+MG recalibration:** 60-restart multistart fit (`cpuset 0-59`) to establish updated sound-horizon calibration anchor values.
2. **Late-time rebasing:** constrained/pilot transfer sweeps are rebased to the updated Planck-like anchor and recompressed into a final relief posterior.
3. **CMB lensing forecasts:** baseline draw-level CAMB projection to Planck 2018 lensing bandpowers, followed by an MG-aware two-parameter lensing refit.
4. **Compressed standard-ruler inversion:** GR inversion of $\theta_* = r_d/D_M(z_*)$ under fixed- Ω_m and lensing-proxy- Ω_m assumptions.

These are targeted forecasts and refits, not a full MG TT/TE/EE perturbation-sector likelihood analysis.

III. RESULTS

A. Updated sound-horizon calibration anchor from the global Planck+MG fit

The 60-restart Planck+MG run completed all restarts with 5 converged minima and 55 max-evaluation exits. Using converged minima only, we obtain:

$$\begin{aligned} H_0^{\text{Planck, MG}} &= 68.01 \text{ (p50),} \\ \Omega_m^{\text{Planck, MG}} &= 0.3064 \text{ (p50),} \\ A_{\text{lens}} &= 1.043 \text{ (p50).} \end{aligned} \quad (1)$$

With local reference $H_0^{\text{local}} = 73.0$, the baseline gap used in rebased relief calculations is

$$\Delta H_0^{\text{base}} = |H_0^{\text{local}} - H_0^{\text{Planck, MG}}| = 4.99. \quad (2)$$

B. Inference bias from GR standard-ruler inversion

To isolate model-assumption bias, we treat MG posterior draws as truth and invert $\theta_* = r_d/D_M(z_*)$ with a GR compression model:

- fixed $\Omega_m = \Omega_m^{\text{Planck, MG}}$: $H_{0,\text{inferred}}$ mean 72.39 (p50 73.17), with mean $\Delta H_0 = +1.88 \text{ km s}^{-1} \text{ Mpc}^{-1}$ relative to draw-level truth;
- lensing-proxy Ω_m : $H_{0,\text{inferred}}$ mean 75.07 (p50 75.23), with mean $\Delta H_0 = +4.55 \text{ km s}^{-1} \text{ Mpc}^{-1}$.

The wider lensing-proxy interval reflects the expected $H_0-\Omega_m$ degeneracy once the artificial rigidity of the ΛCDM standard ruler is removed; in this channel, the analysis releases model-imposed precision rather than exhibiting numerical instability.

Relative to the recalibrated Planck+MG anchor $H_0^{\text{Planck, MG}} = 68.01$, the posterior medians shift by:

$$\begin{aligned} \Delta H_0^{\text{truth}} &\approx +2.39, \\ \Delta H_0^{\text{fixed inversion}} &\approx +5.16, \\ \Delta H_0^{\text{lensing inversion}} &\approx +7.22 \text{ km s}^{-1} \text{ Mpc}^{-1}. \end{aligned} \quad (3)$$

C. Direct friction channel after late-time rebasing

After rebasing constrained transfer sweeps to the updated sound-horizon calibration anchor and applying Monte Carlo calibration:

$$\mathcal{R}_{\text{anchor}}^{\text{GR}} = 0.155. \quad (4)$$

The corresponding posterior summary is p16/p50/p84 = 0.108/0.147/0.189.

Independent robustness and joint-fit diagnostics are:

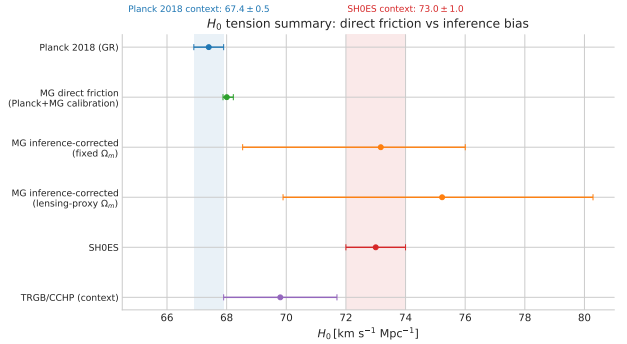


FIG. 1. H_0 tension summary comparing Planck 2018 (GR), direct-friction recalibration, two GR-inversion bias channels, and local-distance-ladder context (SH0ES and TRGB/CCHP [5, 6]). The dominant displacement comes from GR standard-ruler inversion bias when MG truth is assumed; the broad lensing-proxy interval is the expected $H_0-\Omega_m$ degeneracy once the artificial ΛCDM standard-ruler rigidity is relaxed.

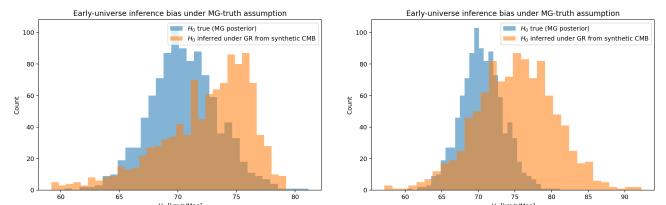


FIG. 2. Draw-level H_0 truth versus GR-inferred H_0 under compressed standard-ruler inversion with fixed- Ω_m (left) and lensing-proxy- Ω_m (right). Both assumptions bias inferred H_0 upward, with larger displacement in the lensing-proxy case.

- 10-case robustness grid: posterior-shift relief mean 0.530 (p50 0.513, p84 0.545), with zero failed cases.
- Joint SN+BAO+CC transfer fit: relief posterior mean 0.833 (p50 0.839), but

$$\log \text{BF}_{\text{transfer/no-transfer}} = -0.53, \quad (5)$$

so explicit transfer terms are not favored in this setup.

The high- z transfer-bias sensitivity map used for calibration has been moved to supplemental material (Fig. S1).

D. CMB lensing: baseline suppression and MG-aware response freedom

Baseline draw-level CAMB projection against Planck 2018 lensing bandpowers (`consext8`, 64 draws) gives:

$$\left. \frac{C_L^{\phi\phi}(\text{MG})}{C_L^{\phi\phi}(\text{Planck ref})} \right|_{L \approx 106} = 0.847^{+0.091}_{-0.127}, \quad (6)$$

$$\left. \frac{C_L^{\phi\phi}(\text{MG})}{C_L^{\phi\phi}(\text{Planck ref})} \right|_{L \approx 286} = 0.905^{+0.068}_{-0.080}, \quad (7)$$

with median suppressions of -15.29% and -9.49% . The baseline fit quality is poor relative to the Planck-reference model:

$$\chi_{\text{MG, baseline}}^2 (\text{median}) = 51.77, \quad \chi_{\text{Planck ref}}^2 = 9.04, \quad (8)$$

and only 3.1% of draws outperform the reference. A 32-draw cross-check from an independent posterior sample is more discrepant (-18.66% at $L \approx 106$, -11.29% at $L \approx 286$; $p_{\text{better}} = 0$).

To test whether this baseline mismatch is rigid, we perform an MG-aware lensing refit (32 draws) with a phenomenological effective- M_\star^2 amplitude plus ℓ -tilt response. This freedom is motivated by scalar-tensor/EFT treatments where matter-growth and light-deflection responses need not track identically and can acquire scale dependence [17, 18]. The refit removes the baseline mismatch:

$$\chi_{\text{MG refit}}^2 (\text{median}) = 8.06, \quad (9)$$

better than the Planck-reference $\chi^2 = 9.04$ in 100% of refit draws. This refit is phenomenological and demonstrates model-class freedom, not a unique derivation of one covariant MG Lagrangian. The fitted median response corresponds to

$$\frac{M_\star^2(z=0)}{M_\star^2(z \gg 1)} \simeq 0.901 \quad (10)$$

(about a 9.9% drop), with small residual suppression at $L \approx 286$.

E. Forward amplitude-dial sensitivity test

To quantify how strongly the reconstructed propagation signal must scale to satisfy forward consistency gates, we ran a lightweight amplitude dial around the current posterior signal:

$$R_\alpha(z) = 1 + \alpha [R(z) - 1]. \quad (11)$$

Using the existing Phase 2–6 gate summaries as a fast emulator (not a full re-inference at each α), we find:

- Phase-4 distance-ratio gate passes at $\alpha \approx 0.18$;
- Phase-2 growth gate passes at $\alpha \approx 0.58$;
- Phase-3 lensing-growth consistency gate passes at $\alpha \approx 0.60$;
- Combined target-support gate (M2) turns on at $\alpha \approx 0.60$.

For the material-relief requirement ($\mathcal{R}_{\text{anchor}}^{\text{GR}} \geq 0.30$), two cases are informative: (i) if relief is held fixed at the current calibrated level, no solution appears for $\alpha \in [0, 3]$; (ii) under linear relief coupling, $\mathcal{R}_{\text{anchor}}(\alpha) \propto \alpha$, the threshold is crossed at $\alpha \approx 1.95$. This points to a simple scale estimate: core cross-channel support is compatible with the present signal level, while material closure needs roughly a factor-of-two stronger effective propagation amplitude under linear coupling.

F. Predictive triplet quick tests (non-waveform)

We then ran three lightweight forward checks designed to test whether the current signal can be embedded in a broader predictive picture without adding new heavy global fits.

Pantheon inference-bias audit. In an SN-only transfer model, we obtain a weak same-sign preference for transfer terms:

$$\log \text{BF}_{\text{transfer/no-transfer}} \approx +0.24. \quad (12)$$

In the all-transfer variant (SN+BAO+CC+ladder term), the score is mildly negative:

$$\log \text{BF}_{\text{transfer/no-transfer}} \approx -0.48. \quad (13)$$

This is compatible with a small inference-bias contribution in SN-only compression, but not a decisive multi-probe detection at current calibration depth.

Hero-event concentration forensics. For the O3 injection-logit configuration, the full score is

$$\Delta \text{LPD}_{\text{full}} = 3.67. \quad (14)$$

Dropping the highest-leverage event (GW200308_173609) gives

$$\Delta \text{LPD}_{\text{drop 1}} = 2.19, \quad (15)$$

and an approximate top-2 leave-out gives

$$\Delta \text{LPD}_{\text{drop 2}} \approx 1.70. \quad (16)$$

So the signal is concentrated in a small subset, but it does not collapse when the top event is removed.

Nonlinear bridge scan. Using a late-transition profile

$$\alpha(z) = \alpha_{\text{high}} + \frac{\alpha_{\text{low}} - \alpha_{\text{high}}}{1 + \exp[(z - z_t)/w]}, \quad (17)$$

we find broad viable families that satisfy the core gates ($\alpha_{\text{eff}} \sim 0.6$ in the growth/lensing windows) while reaching material-relief targets ($\alpha_{\text{relief,eff}} \sim 1.94$ to 1.95 in low- z windows). A representative solution is

$$(\alpha_{\text{high}}, \alpha_{\text{low}}, z_t, w) \approx (0.60, 1.95, 0.26, 0.03), \quad (18)$$

with comparable neighboring solutions for other low- z effective windows.

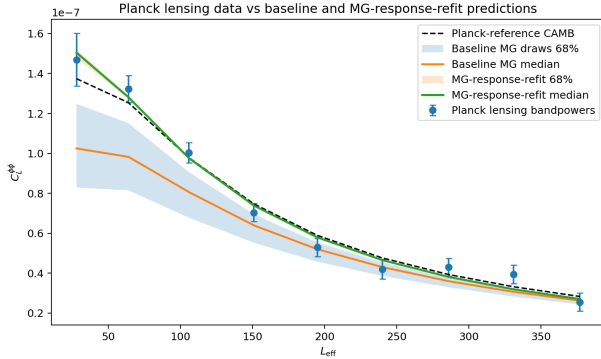


FIG. 3. Planck 2018 lensing bandpowers with baseline MG projection and MG-aware refit overlay. The refit absorbs the baseline suppression and restores near-reference fit quality.

IV. DISCUSSION AND CONCLUSION

The main implication is that inference bias from GR-assumed standard-ruler inversion can be cosmologically large if the O3 modified-propagation posterior corresponds to physical MG truth. In this pipeline, that channel displaces recovered H_0 by order +2 to +5 km s $^{-1}$ Mpc $^{-1}$ relative to draw-level truth, with larger shifts relative to the recalibrated Planck+MG anchor.

The direct friction channel remains subdominant in the constrained rebased analysis: $\mathcal{R}_{\text{anchor}}^{\text{GR}} \simeq 0.16$. This means the principal lever in this study is model-assumption bias from GR-assumed standard-ruler inversion, not direct late-time closure alone.

For CMB lensing, baseline propagation is strongly discrepant with Planck 2018. An MG-aware response refit motivated by effective-coupling freedom in scalar-tensor/EFT descriptions restores near-reference likelihood performance. If that response freedom is not permitted, the baseline projection remains in strong tension with lensing data.

The new predictive triplet checks sharpen this interpretation. Pantheon SN-only transfer is weakly positive while all-transfer remains mildly negative, consistent with directional compatibility but not decisive closure. Hero-event forensics show concentration in GW200308_173609 and a small set of high-leverage events, but no single-event collapse. The nonlinear bridge scan shows that late-time transition families can satisfy both sets of requirements simultaneously: core gate consistency near $\alpha \sim 0.6$ and material-relief scale near $\alpha \sim 2$.

Taken together, these results recast the follow-up question from “does friction alone close the full tension?” to “how much of the inferred early-versus-late mismatch can come from GR-compression bias plus late-time transition structure when MG truth is present?” This scale should be tested directly with full re-inference as larger siren samples arrive.

REPRODUCIBILITY

Core scripts used in this follow-up are:

- `scripts/run_planck_global_mg_refit_multistart.py`
- `scripts/rebase_bias_transfer_sweep_to_planck_ref.py`
- `scripts/run_hubble_tension_final_relief_posterior.py`
- `scripts/run_hubble_tension_mg_forecast_robustness_grid.py`
- `scripts/run_joint_transfer_bias_fit.py`
- `scripts/run_hubble_tension_cmb_forecast.py`
- `scripts/run_hubble_tension_mg_lensing_refit.py`
- `scripts/run_hubble_tension_early_universe_bias.py`
- `scripts/run_forward_tests_signal_amplitude_dial.py`
- `scripts/run_forward_tests_nonlinear_bridge_quick.py`

ACKNOWLEDGMENTS

This work used A.I. tools extensively, including ChatGPT 5.3.

DATA AVAILABILITY AND DOIS

The follow-up uses posterior products from the O3 anomaly pipeline and public cosmology datasets. Data provenance and DOIs are:

- O3 modified-gravity tension anomaly repository (Zenodo): DOI 10.5281/zenodo.18585598.

- O3 search-sensitivity injection data used in upstream calibration (Zenodo): DOI 10.5281/zenodo.7890437.
- GWTC-3 catalog paper: DOI 10.1103/PhysRevX.13.041039.
- Pantheon+ cosmology constraints: DOI 10.3847/1538-4357/ac8e04.
- SH0ES local- H_0 reference: DOI 10.3847/2041-8213/ac5c5b.
- TRGB/CCHP local- H_0 context reference: DOI 10.3847/1538-4357/ab2f73.
- SDSS DR12 BOSS consensus BAO (source of `sdss_DR12Consensus_bao.dat`): DOI 10.1093/mnras/stx721.
- eBOSS DR16 cosmological compilation (source class for `sdss_DR16_LRG_BAO_DMDH.dat`): DOI 10.1103/PhysRevD.103.083533.
- DESI 2024 BAO cosmological constraints (source class for `desi_2024_gaussian_bao_ALL_GCcomb_mean.txt`): DOI 10.1088/1475-7516/2025/02/021.
- Cosmic-chronometer compilation components used in `Hz_BC03_all.dat`: DOIs 10.1088/1475-7516/2012/08/006, 10.1103/PhysRevD.71.123001, and 10.1088/1475-7516/2010/02/008.
- Planck 2018 cosmological-parameter and lensing references: DOIs 10.1051/0004-6361/201833910 and 10.1051/0004-6361/201833886.

-
- [1] A. B. Smith, “O3 Modified Gravity Tension Replication,” Zenodo (2026), DOI: 10.5281/zenodo.18585598.
- [2] LIGO Scientific Collaboration, Virgo Collaboration, and KAGRA Collaboration, “GWTC-3: Compact Binary Coalescences Observed by LIGO and Virgo During the Second Part of the Third Observing Run — O3 search sensitivity estimates,” Zenodo (2023), DOI: 10.5281/zenodo.7890437.
- [3] R. Abbott *et al.* (LIGO Scientific Collaboration, Virgo Collaboration, and KAGRA Collaboration), “GWTC-3: Compact Binary Coalescences Observed by LIGO and Virgo During the Second Part of the Third Observing Run,” *Phys. Rev. X* **13**, 041039 (2023), DOI: 10.1103/PhysRevX.13.041039.
- [4] D. Brout *et al.*, “The Pantheon+ Analysis: Cosmological Constraints,” *Astrophys. J.* **938**, 110 (2022), DOI: 10.3847/1538-4357/ac8e04.
- [5] A. G. Riess *et al.*, “A Comprehensive Measurement of the Local Value of the Hubble Constant with $1 \text{ km s}^{-1} \text{ Mpc}^{-1}$ Uncertainty from the Hubble Space Telescope and the SH0ES Team,” *Astrophys. J. Lett.* **934**, L7 (2022), DOI: 10.3847/2041-8213/ac5c5b.
- [6] W. L. Freedman *et al.*, “The Carnegie-Chicago Hubble Program. VIII. An independent determination of the Hubble constant based on the tip of the red giant branch,” *Astrophys. J.* **882**, 34 (2019), DOI: 10.3847/1538-4357/ab2f73.
- [7] S. Alam *et al.*, “The clustering of galaxies in the com-

- pleted SDSS-III Baryon Oscillation Spectroscopic Survey: cosmological analysis of the DR12 galaxy sample,” *Mon. Not. R. Astron. Soc.* **470**, 2617 (2017), DOI: 10.1093/mnras/stx721.
- [8] S. Alam *et al.*, “Completed SDSS-IV extended Baryon Oscillation Spectroscopic Survey: Cosmological implications from two decades of spectroscopic surveys at the Apache Point Observatory,” *Phys. Rev. D* **103**, 083533 (2021), DOI: 10.1103/PhysRevD.103.083533.
- [9] DESI Collaboration, “DESI 2024 VI: cosmological constraints from the measurements of baryon acoustic oscillations,” *J. Cosmol. Astropart. Phys.* **02** (2025) 021, DOI: 10.1088/1475-7516/2025/02/021.
- [10] M. Moresco *et al.*, “Improved constraints on the expansion rate of the Universe up to $z \sim 1.1$ from the spectroscopic evolution of cosmic chronometers,” *J. Cosmol. Astropart. Phys.* **08** (2012) 006, DOI: 10.1088/1475-7516/2012/08/006.
- [11] J. Simon, L. Verde, and R. Jimenez, “Constraints on the redshift dependence of the dark energy potential,” *Phys. Rev. D* **71**, 123001 (2005), DOI: 10.1103/PhysRevD.71.123001.
- [12] D. Stern *et al.*, “Cosmic chronometers: constraining the equation of state of dark energy. I: $H(z)$ measure-
- ments,” *J. Cosmol. Astropart. Phys.* **02** (2010) 008, DOI: 10.1088/1475-7516/2010/02/008.
- [13] N. Aghanim *et al.* (Planck Collaboration), “Planck 2018 results. VI. Cosmological parameters,” *Astron. Astrophys.* **641**, A6 (2020), DOI: 10.1051/0004-6361/201833910.
- [14] N. Aghanim *et al.* (Planck Collaboration), “Planck 2018 results. VIII. Gravitational lensing,” *Astron. Astrophys.* **641**, A8 (2020), DOI: 10.1051/0004-6361/201833886.
- [15] E. Belgacem, Y. Dirian, S. Foffa, and M. Maggiore, “Modified gravitational-wave propagation and standard sirens,” *Phys. Rev. D* **98**, 023510 (2018), DOI: 10.1103/PhysRevD.98.023510.
- [16] A. Nishizawa, “Generalized framework for testing gravity with gravitational-wave propagation,” *Phys. Rev. D* **97**, 104037 (2018), DOI: 10.1103/PhysRevD.97.104037.
- [17] E. Bellini and I. Sawicki, “Maximal freedom at minimum cost: linear large-scale structure in general modifications of gravity,” *J. Cosmol. Astropart. Phys.* **07** (2014) 050, DOI: 10.1088/1475-7516/2014/07/050.
- [18] L. Pogosian and A. Silvestri, “What can cosmology tell us about gravity? Constraining Horndeski gravity with Σ and μ ,” *Phys. Rev. D* **94**, 104014 (2016), DOI: 10.1103/PhysRevD.94.104014.